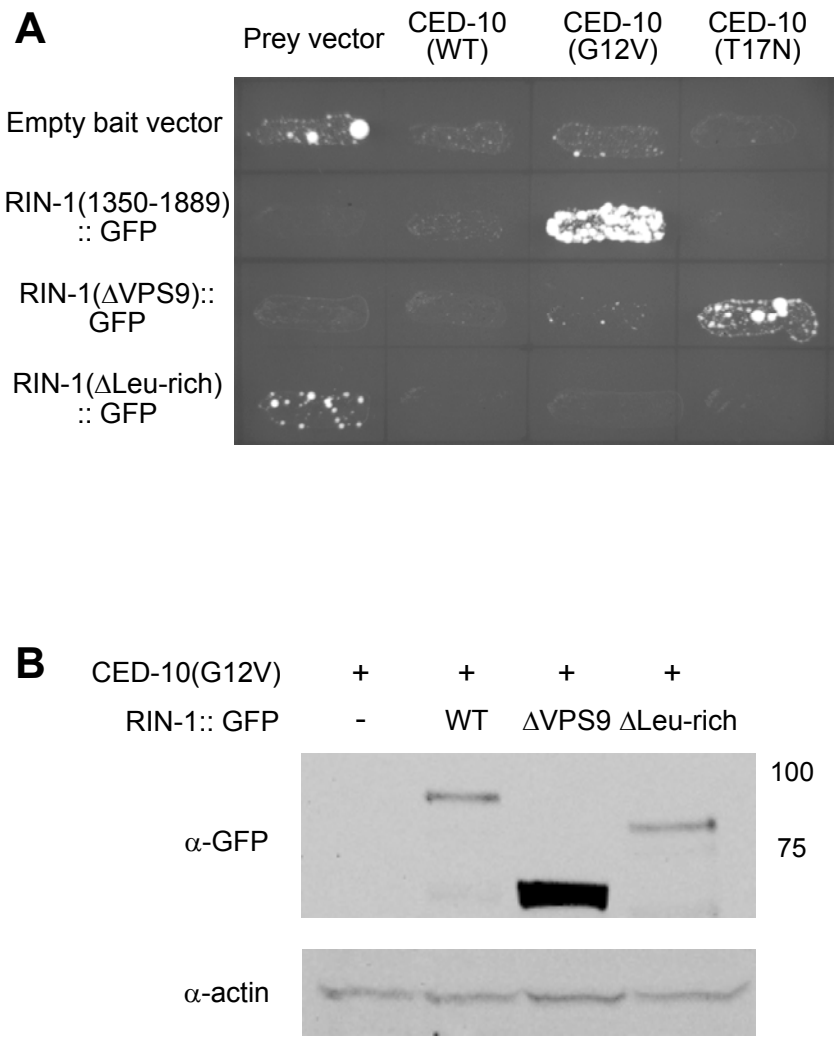

Fig. S1. Expression of GFP-fused RIN-1 mutant proteins in the yeast used for the two-hybrid analysis. (**A**) Interaction between CED-10 and each GFP-fused RIN-1 protein. As with Fig. 1B, only the wild-type RIN-1::GFP fusion protein strongly interacted with the constitutively active form of CED-10(G12V). (**B**) Western blotting of RIN-1::GFP fusion proteins. Transformed yeast cell lysates were analyzed by immunoblot with anti-GFP. The predicted molecular weight of each fusion protein was 87 kDa for the wild-type RIN-1 C-terminal fragment, 57 kDa for the ΔVPS form, and 79 kDa for the ΔLeu-rich form. Note that both the ΔVPS and ΔLeu-rich mutant forms were expressed stably and comparably to the wild-type RIN-1 C-terminal fragment. An anti-actin antibody (Chemicon) was used as a loading control.

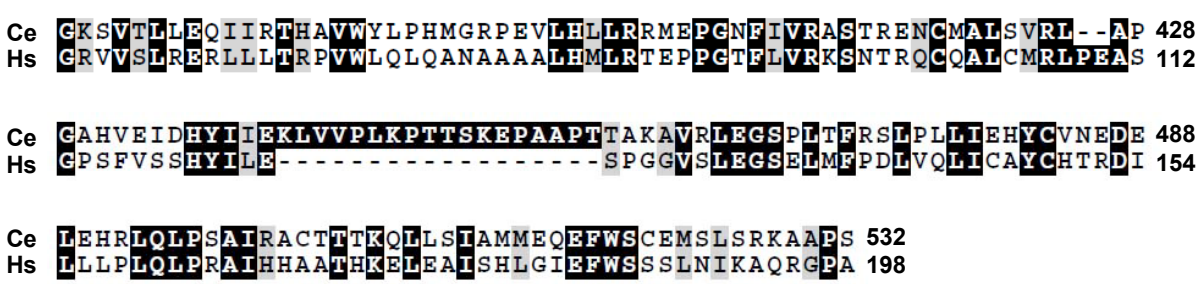

Fig. S2. Amino acid alignment between the SH2 domain of *C. elegans* RIN-1 and human RIN1. Ce, *C. elegans* RIN-1; Hs, human RIN1. Black indicates identical amino acids and gray similar amino acids. The SH2 domains of the two proteins show 35% identity and 47% similarity.

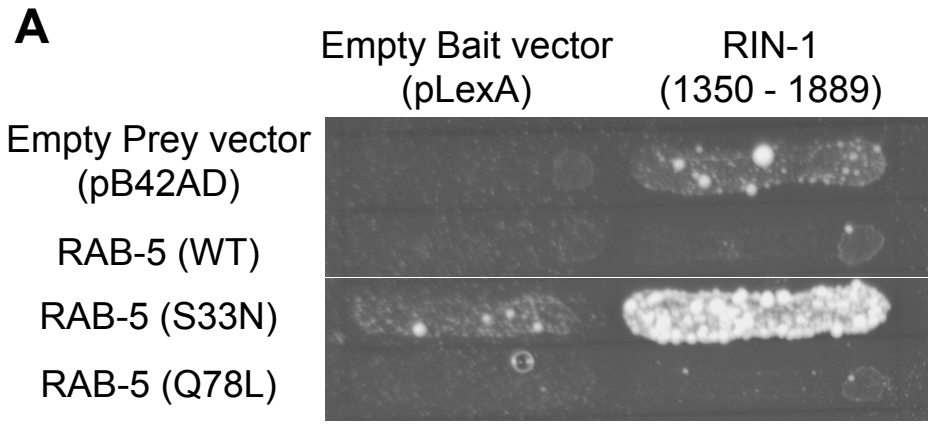

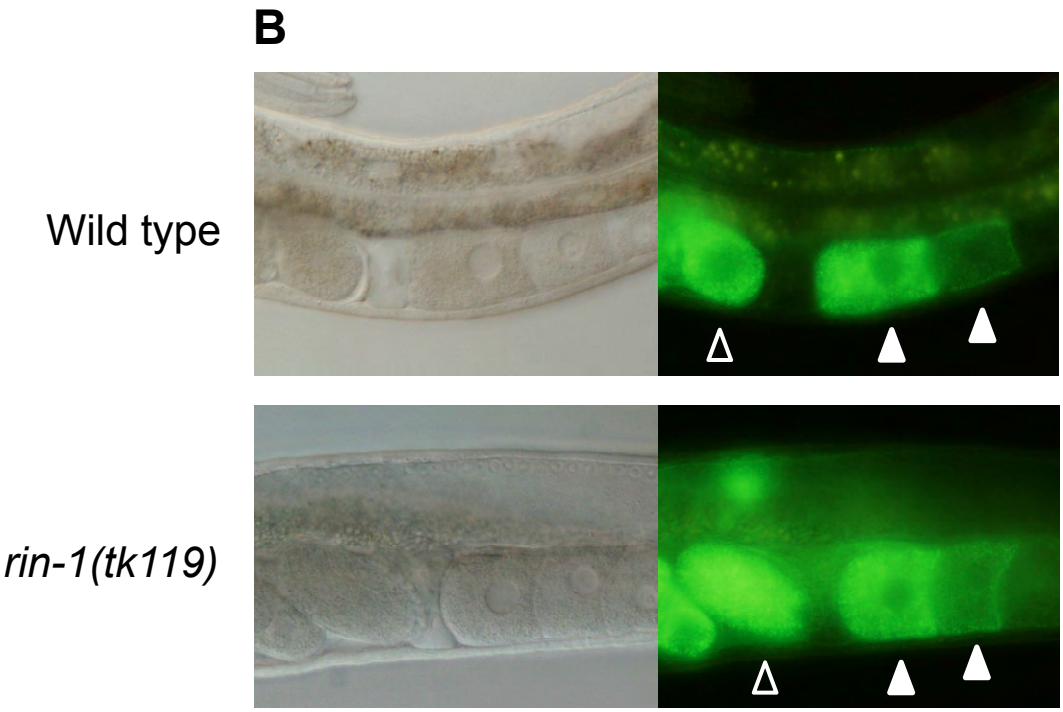

Fig. S3. RIN-1 interacts with GDP-bound RAB-5 but does not appear to regulate RAB-5 activity. (**A**) Yeast two-hybrid assay of the C-terminal region of RIN-1 and RAB-5. See Fig. 1 for the RIN-1 region used for this assay. The S33N mutation locks RAB-5 into the GDP-bound form, and the Q78L mutation into the GTP-bound form. Positive interaction between RIN-1 and RAB-5(S33N), the GDP-bound form, suggests that RIN-1 may function as a RAB-5 GEF. (**B**) Receptor-mediated endocytosis of a yolk protein was unchanged in *rin-1* mutants. A transgene (*bIs1*) encoding the yolk protein vitellogenin fused to GFP (VIT-2::GFP) was introduced into *rin-1* mutants. This transgene is widely used to examine endocytic functions in genes of interest (Grant and Hirsh, 1999). Left, DIC image; right, GFP image. The fusion protein is secreted from intestinal cells and is endocytosed by mature oocytes (closed arrowheads). GFP fluorescence was also observed in fertilized embryos (open arrowhead). Upper panel, wild type; lower panel, *rin-1(tk119)* mutant. Note that a clear GFP signal was present in the *rin-1* mutant oocytes. Similar results were obtained using *rin-1(gk431)* mutants, suggesting that receptor-mediated endocytosis is not altered in existing *rin-1* mutant alleles.

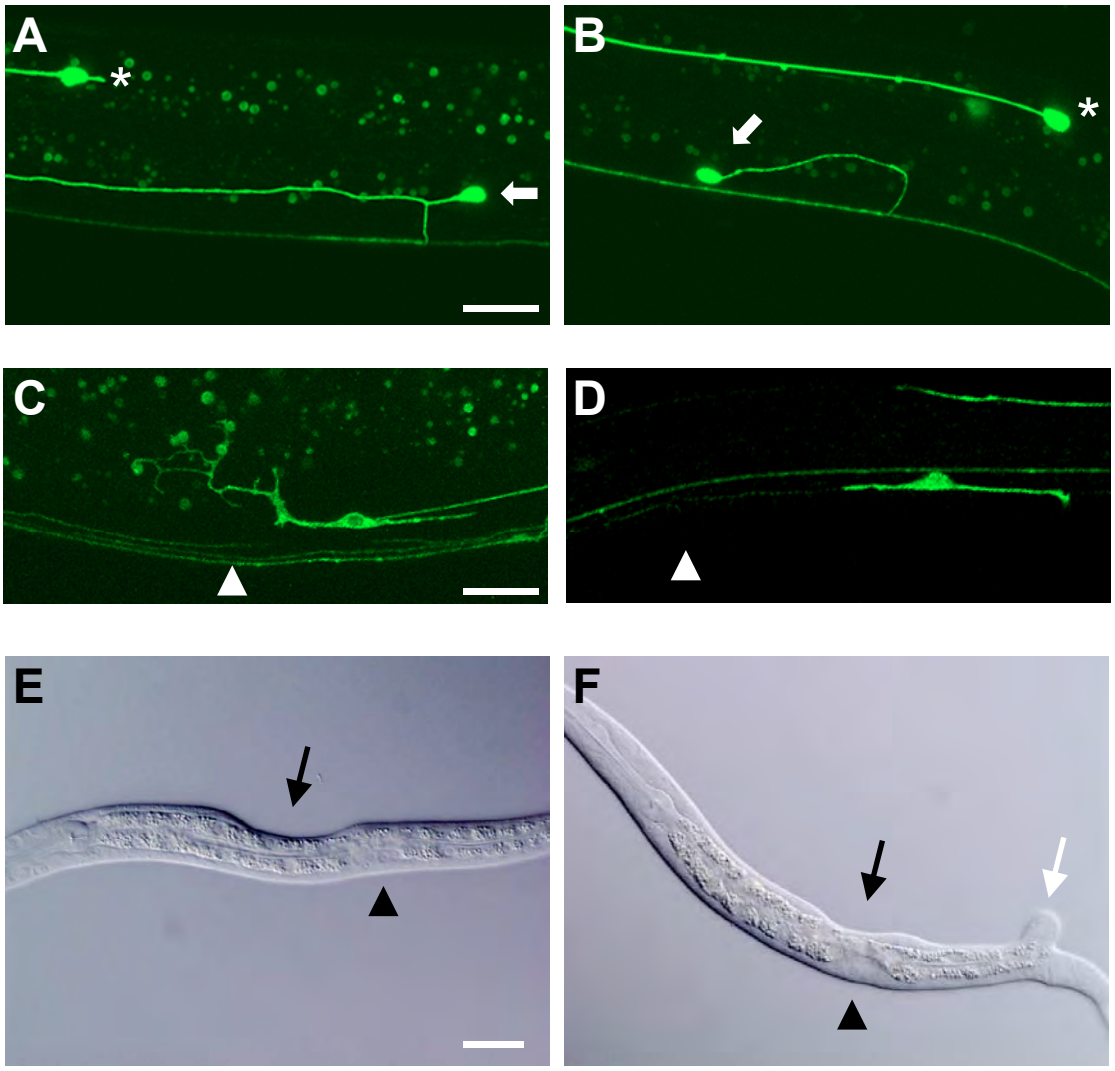

Fig. S4. Examples of defective phenotypes in *rin-1; mig-2* mutants. (**A**,**B**) AVM axon guidance. Arrow indicates the AVM neuron, asterisk indicates the ALM neuron. (**C**,**D**) HSN axon guidance. Arrowheads indicate the position of the vulva. (**E**,**F**) Dorsal morphology of L1 larva. Dorsal collapse (black arrow) and protrusion (white arrow) were observed. Position of the vulva is indicated by the arrowhead. Scale bars: 10 μm.

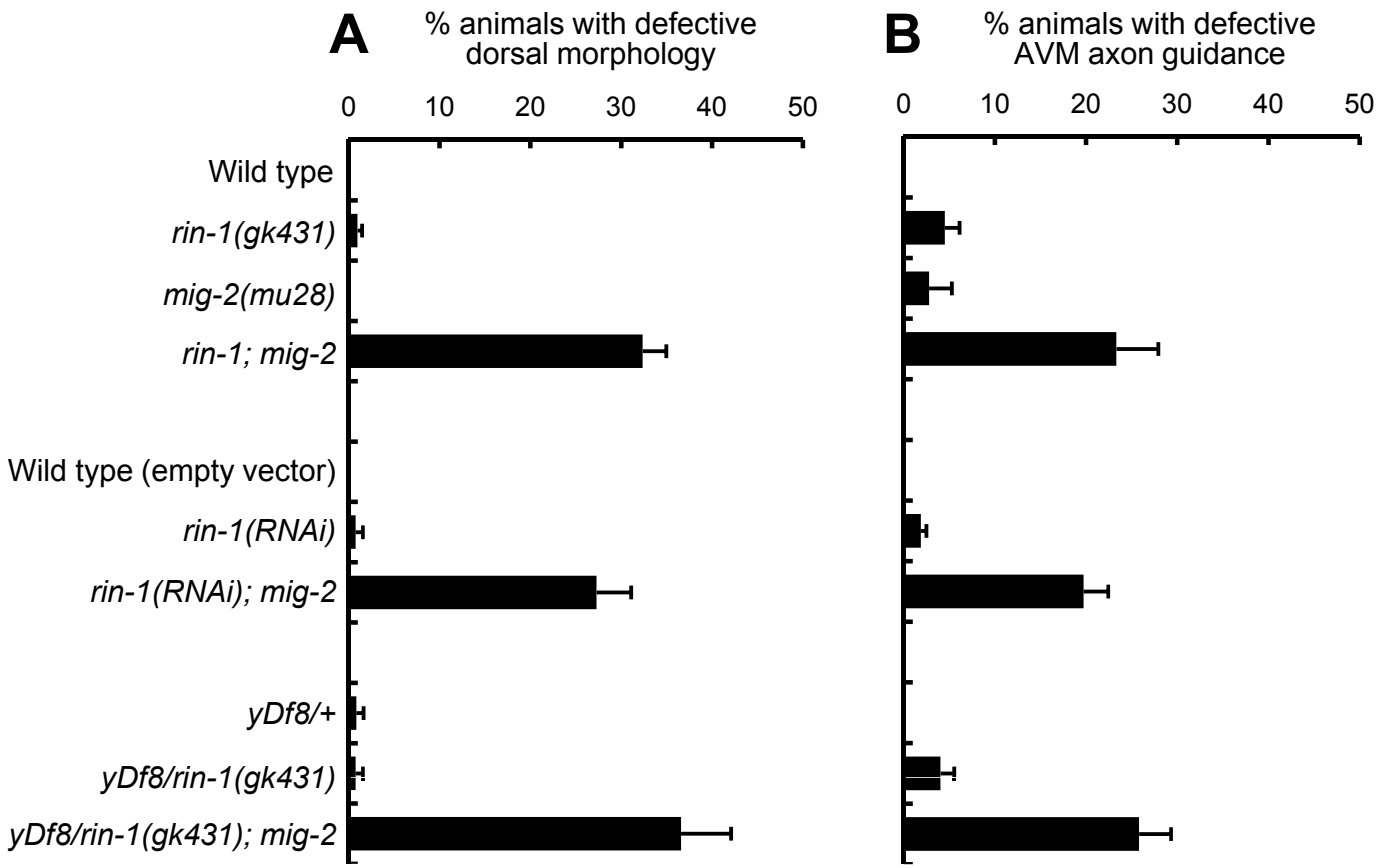

Fig. S5. Characterization of the *rin-1* mutant allele. Dorsal morphology (**A**) and AVM axon guidance (**B**) were observed in the *rin-1* knockdown animal by feeding RNAi and in transheterozygous animals between *rin-1(gk431)* and the *yDf8* deficiency. To increase the sensitivity to neuronal RNAi, all the strains used for RNAi experiments bear the *uIs69* transgene (integrated *Punc-119::sid-1*) (Calixto et al., 2010). *rin-1(RNAi); mig-2* animals showed similar defects to *rin-1(gk431); mig-2* animals, suggesting that the *gk431* allele is a loss-of-function mutation. The *yDf8* deficiency lacks the region from map position 6.1 to 10.3 on chromosome V, within which *rin-1* (map position 6.8) is located. The transheterozygous animals showed a small increase in penetrance compared with the *rin-1(gk431); mig-2* double-mutant animals. This also suggests that the *gk431* allele is a strong loss-of-function mutation. All of the genetic analyses with the *yDf8* deficiency were carried out using strains bearing the *zdIs5* transgene.

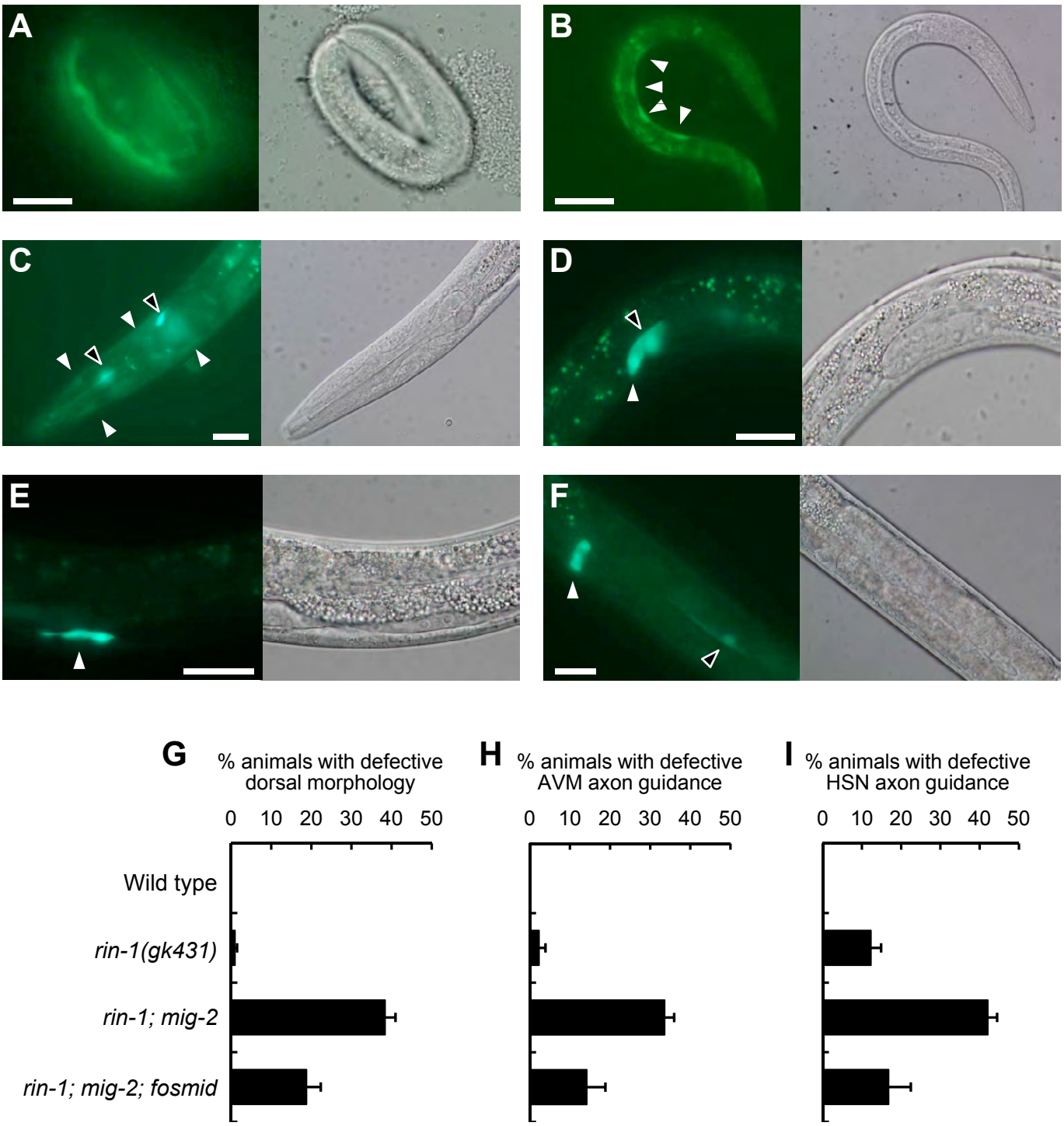

Fig. S6. Expression patterns of *rin-1* and rescue by the fosmid clone. (**A-F**) Expression patterns of a transcriptional reporter gene. A 2.0 kb promoter region was fused to GFP and was expressed in wild-type animals. (A) Three-fold embryo. (B) L1 stage. Weak GFP signal is observed in body wall muscle cells (arrowheads), but was not observed at later stages. (C) Head region of L1 stage. GFP is expressed in several neurons (open arrowheads) and weakly in the hypodermis (closed arrowheads). (D) L2 stage. Distal tip cell (closed arrowhead) and somatic gonad (open arrowhead) expressed GFP. Expression in the posterior DTC was faint in this animal. (E) L3 stage. GFP is observed in the uterus. (F) L4 stage. From L4 to adult stages, GFP was mainly observed in spermatheca (closed arrowhead) and gonadal sheath cells (open arrowhead), and expression in other tissues was very rare. Scale bars: 10 μm. (**G-I**) Rescue of the *rin-1* defects by the whole *rin-1* genomic region. Transgenic animals bearing the *C. elegans* fosmid clone WRM0626bB06, which contains the whole *rin-1* genomic region, were generated and examined for rescue of the defective *rin-1* phenotypes. (G) Dorsal morphology of L1 larva, (H) AVM axon guidance, (I) HSN axon guidance. The transgene retained all the defective phenotypes observed in the *rin-1; mig-2* double-mutant animals, suggesting that *rin-1* is probably expressed in the AVM and HSN neurons.

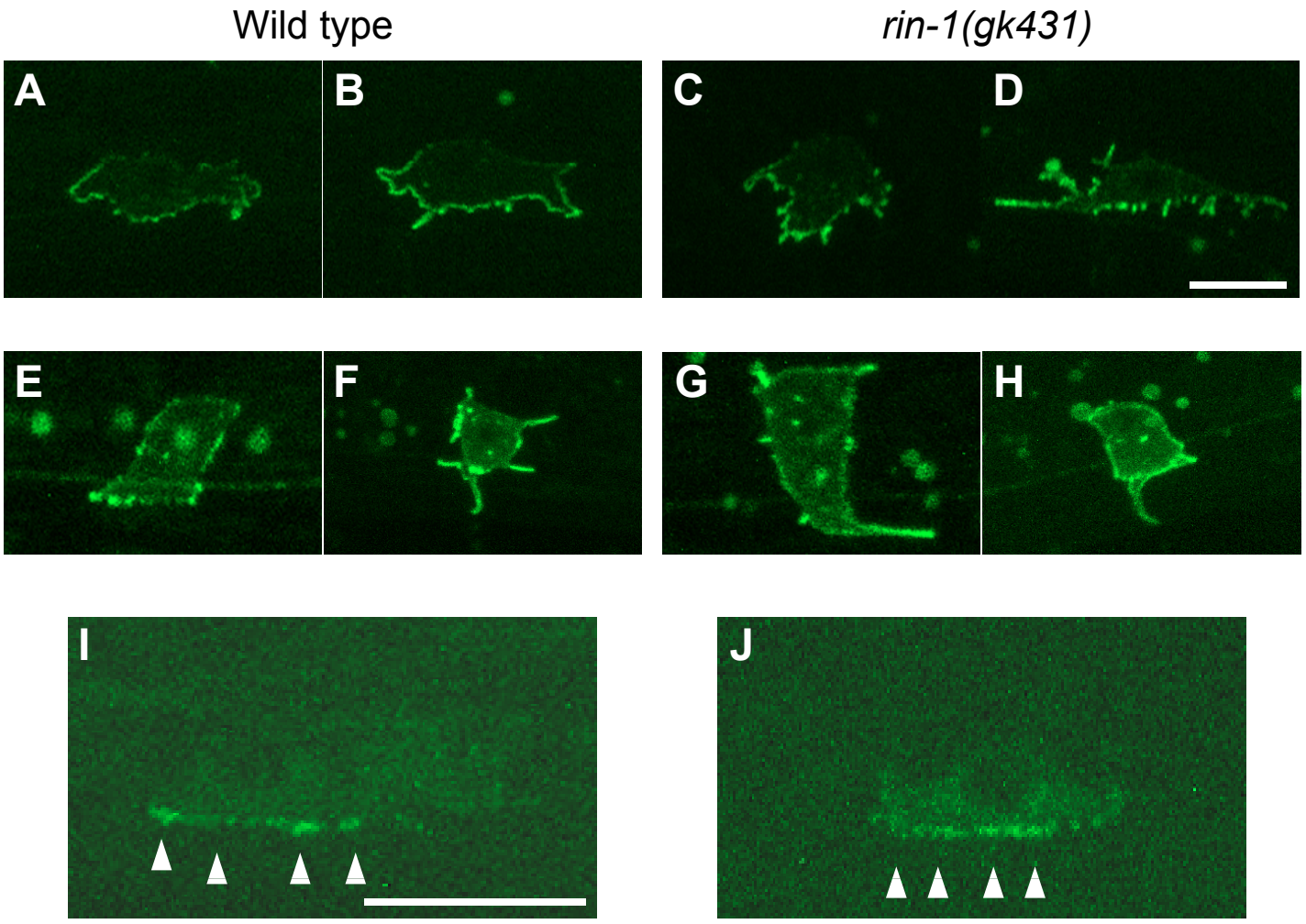

Fig. S7. Localization patterns of guidance receptors and signaling molecules in the developing HSN neuron (L3 stage). The netrin receptor UNC-40, lamellipodin MIG-10 and slit receptor SAX-3 were fused to GFP and were expressed in the HSN neuron using an *unc-86* promoter. (**A-D**) Localization patterns of the UNC-40::GFP fusion protein. The *kyEx1212* transgene was introduced into wild-type (A,B) and *rin-1(gk431)* mutant (C,D) animals. The UNC-40 fusion protein was observed on the ventral side of the cells. No gross differences were observed between the wild type and *rin-1* mutants. (**E-H**) Localization patterns of SAX-3::GFP fusion protein in the HSN neuron of the wild type (E,F) and *rin-1(gk431)* mutant (G,H). The GFP signal was observed at the periphery of the cell body and was especially concentrated in the filopodia-like structures. No gross differences were observed between the wild-type and *rin-1* mutant animals. (**I**,**J**) Localization patterns of the MIG-10::YFP fusion protein. The *kyEx926* transgene was introduced into wild-type (I) and *rin-1* mutant (J) animals. MIG-10 was also localized on the ventral side, but within a more restricted region of the cells.